Supplementary Information for

Tautomeric Mixture Coordination Enables Efficient Lead-Free Perovskite LEDs

Dongyuan Han[1#], Jie Wang[1#], Lorenzo Agosta[2], Ziang Zang[1], Bin Zhao[1], Lingmei Kong[3], Haizhou Lu[4,5]*, Irea Mosquera-Lois[2], Virginia Carnevali[2], Jianchao Dong[1], Jianheng Zhou[1], Huiyu Ji[1], Lukas Pfeifer[4], Shaik M. Zakeeruddin[4], Yingguo Yang[6,7], Bo Wu[8], Ursula Rothlisberger[2], Xuyong Yang[3]*, Michael Grätzel[4]*, Ning Wang[1]*

[1]College of Physics, Jilin University, Changchun, China.
[2]Laboratory of Computational Chemistry and Biochemistry, Institute of Chemical Sciences and Engineering, École Polytechnique Fédérale de Lausanne (EPFL), Lausanne, Switzerland.
[3]Key Laboratory of Advanced Display and System Applications of Ministry of Education, Shanghai University, Shanghai, China.
[4]Laboratory of Photonics and Interfaces, Institute of Chemical Sciences and Engineering, École Polytechnique Fédérale de Lausanne (EPFL), Lausanne, Switzerland.
[5]SEU-FEI Nano-Pico Center, Key Laboratory of MEMS of Ministry of Education, School of Electronics Science and Engineering, Southeast University, Nanjing, China.
[6]Shanghai Synchrotron Radiation Facility (SSRF), Zhangjiang Lab, Shanghai Advanced Research Institute, Chinese Academy of Sciences, Shanghai, China.
[7]School of Microelectronics, Fudan University, Shanghai, China.
[8]Guangdong Provincial Key Laboratory of Optical Information Materials and Technology and Institute of Electronic Paper Displays, South China Academy of Advanced Optoelectronics, South China Normal University, Guangzhou, China.

[#]These authors contributed equally to this work.
*Correspondence to: haizhou.lu@epfl.ch; yangxy@shu.edu.cn; michael.graetzel@epfl.ch; ningwang@jlu.edu.cn.

This file includes:

Supplementary Fig. 1 | FTIR spectra of CA and perovskite thin films.
Supplementary Fig. 2 | XPS spectra of perovskite thin films.
Supplementary Fig. 3 | Planar-averaged electrostatic potential of the perovskites.
Supplementary Fig. 4 | SEM and EDS mapping images of perovskite thin film with CA.
Supplementary Fig. 5 | GIWAXS images of perovskite thin films.
Supplementary Fig. 6 | Surface potential histograms of perovskite thin films.
Supplementary Fig. 7 | Pseudo-color maps of time-dependent PL spectra.
Supplementary Fig. 8 | Photographs of perovskite films.
Supplementary Fig. 9 | Curves of nonradiative capture coefficients with temperature.
Supplementary Fig. 10 | XRD patterns of perovskite thin films for different storage time.
Supplementary Fig. 11 | TA signals and kinetic traces of perovskite thin films.
Supplementary Fig. 12 | Normalized EL spectra of the devices.
Supplementary Fig. 13 | UPS plots of perovskite thin films.
Supplementary Fig. 14 | SCLC analysis.
Supplementary Table 1 | Interaction energy of dimers and trimers.
Supplementary Table 2 | Comparison of Bader charge transfer.
Supplementary Table 3 | Summary of the XPS results for perovskite films.

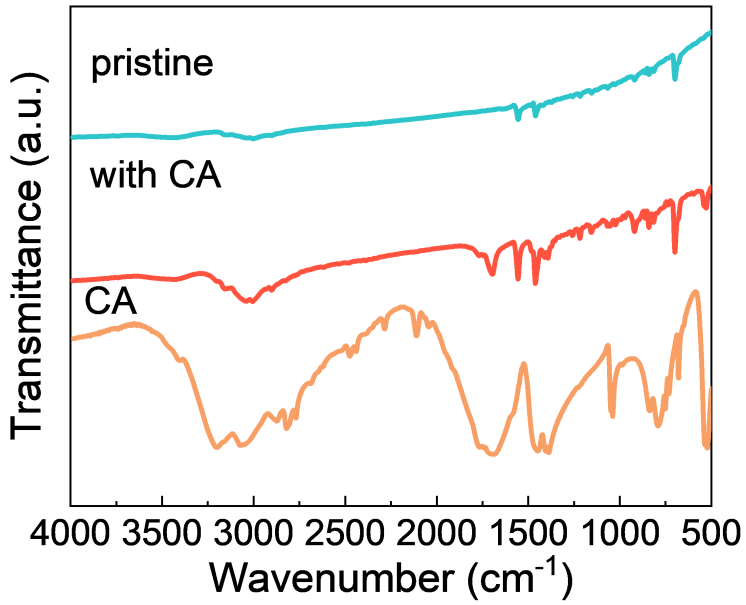

Supplementary Fig. 1 | FTIR spectra of the pure CA and the perovskite thin films. FTIR spectra of the TEA_2SnI_4 films with and without CA treatment, and the pure CA.

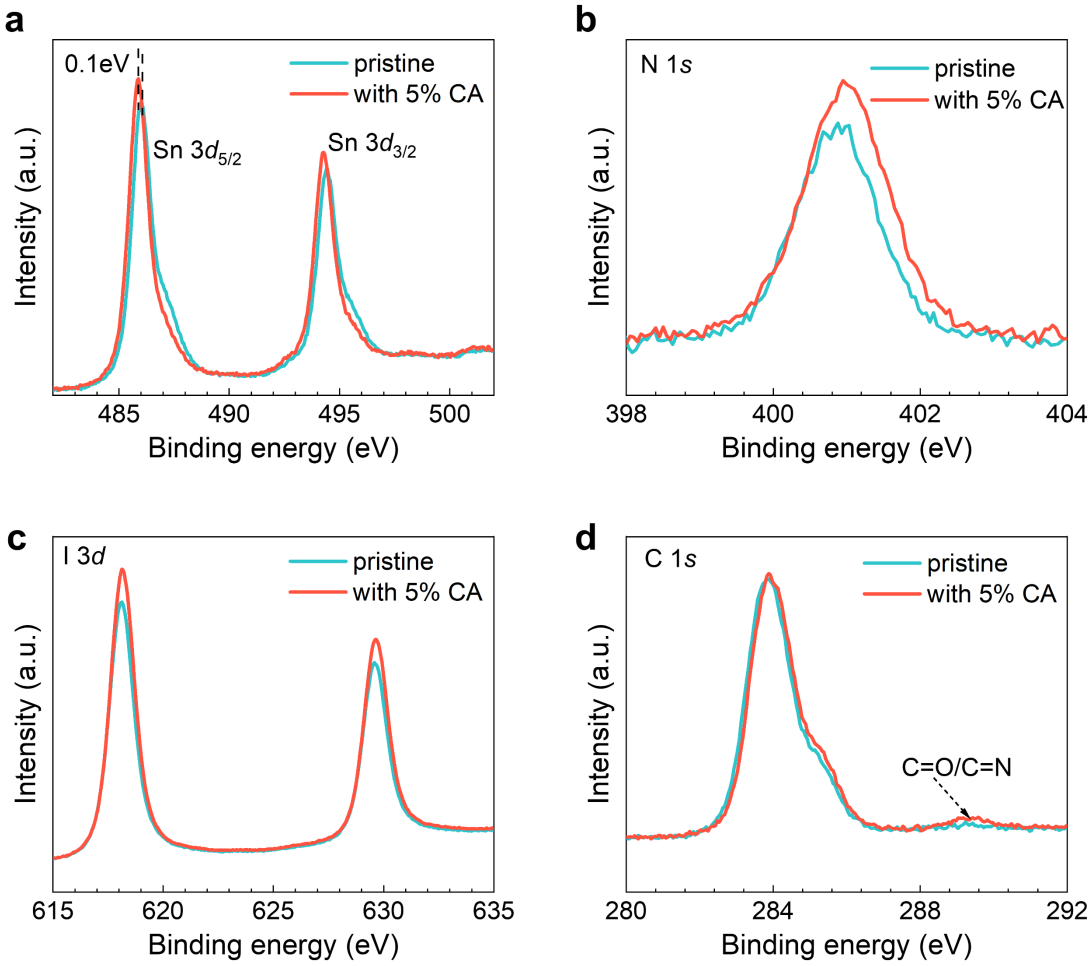

Supplementary Fig. 2 | XPS spectra of the perovskite thin films. Sn 3*d* (**a**), N 1*s* (**b**), I 3*d* (**c**) and C 1*s* (**d**) for the Sn perovskite films with and without 5% CA.

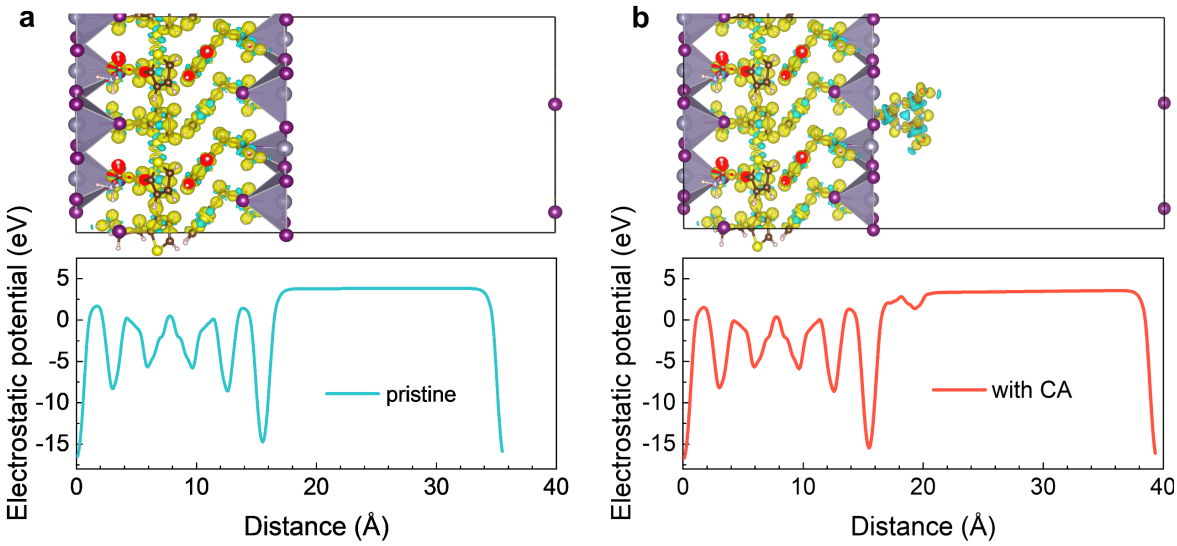

Supplementary Fig. 3 | Planar-averaged electrostatic potential of the perovskites. Planar-averaged electrostatic potential as a function of distance (Å) from the bottom to the top vacuum layer for the pristine (**a**) and the sample with CA (**b**), which are obtained in systems with an iodide vacancy.

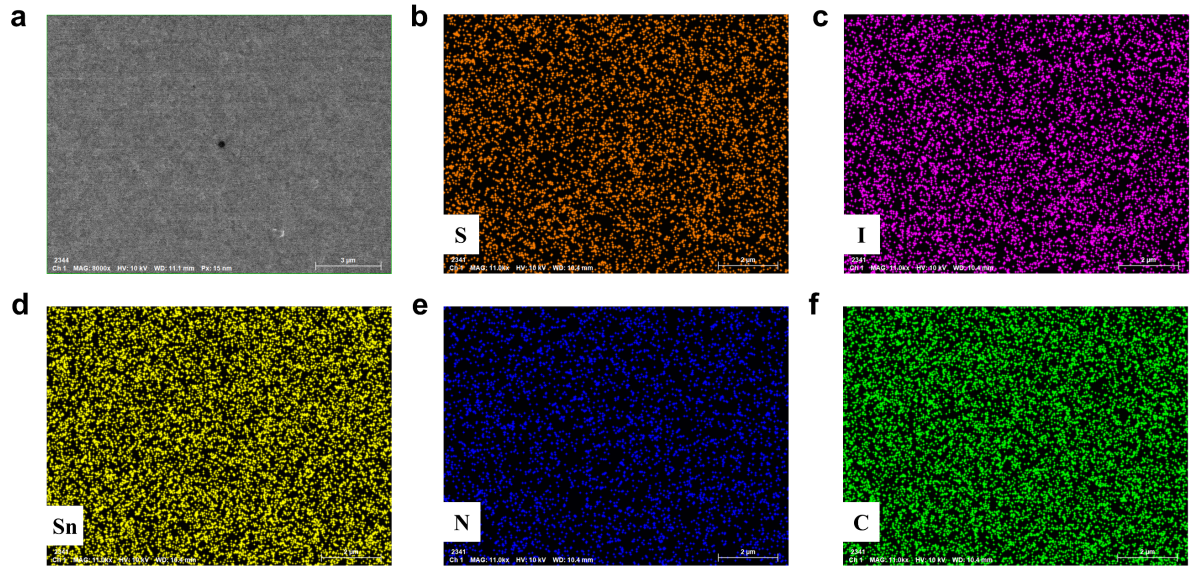

Supplementary Fig. 4 | SEM and EDS mapping images of the perovskite thin film with CA. SEM image (**a**) and the corresponding EDS mapping images of sulfur (**b**), iodine (**c**), tin (**d**), nitrogen (**e**) and carbon (**f**) elements.

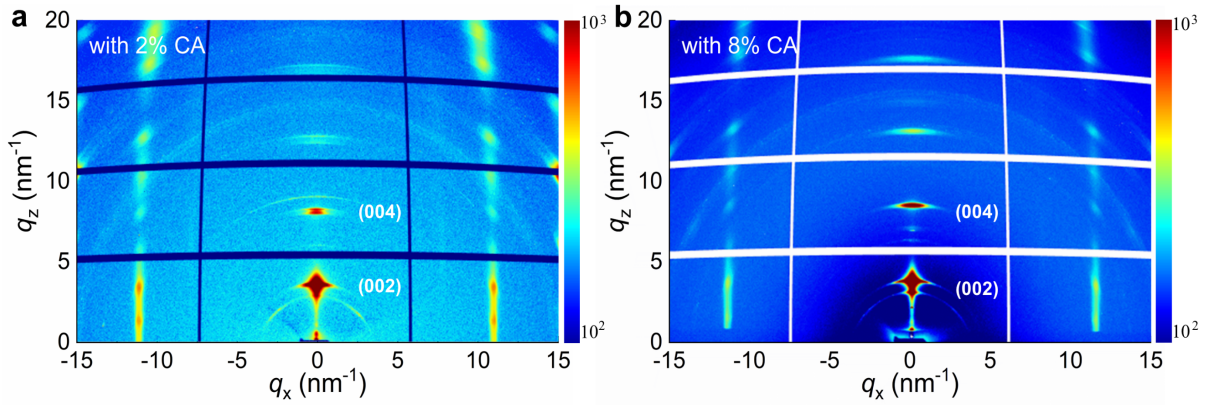

Supplementary Fig. 5 | GIWAXS images of the perovskite thin films. GIWAXS images of TEA_2SnI_4 perovskite films with 2% CA (**a**) and 8% CA (**b**).

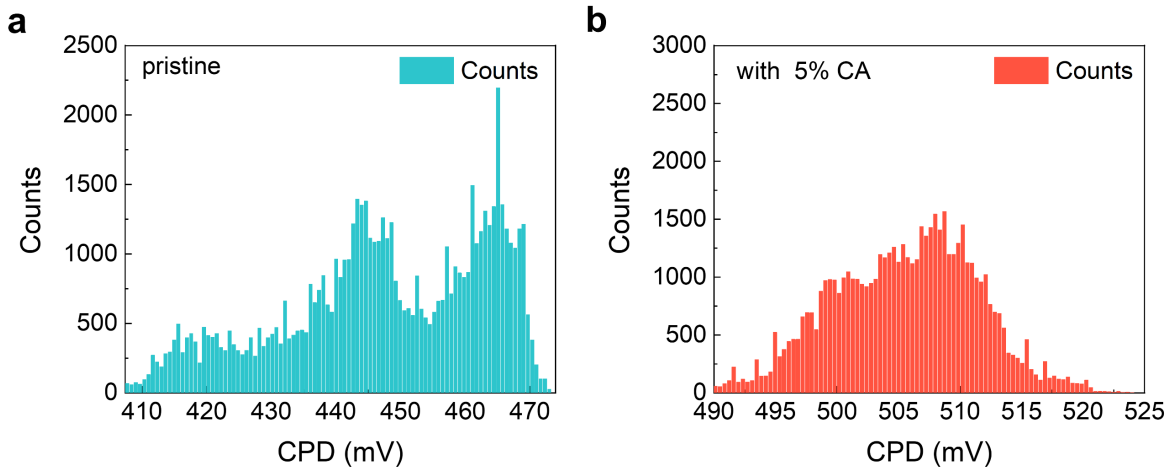

Supplementary Fig. 6 | Surface potential histograms of the perovskite thin films obtained by KPFM. Surface potential histograms for the pristine (**a**) and the 5% CA-treated sample (**b**).

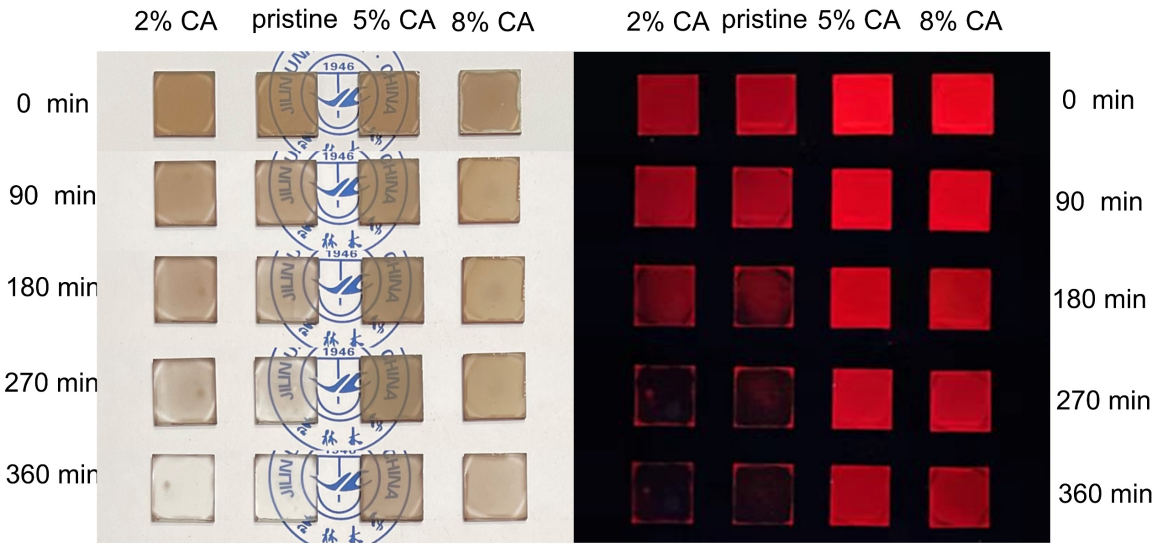

Supplementary Fig. 7 | Photographs of Sn perovskite films. Photographs of Sn perovskite films with different ratios of CA for different storage time in dry air at RT. The right part is the photos of samples in dark with an excitation wavelength of 365 nm, and the left is the photos of samples in dry air without excitation.

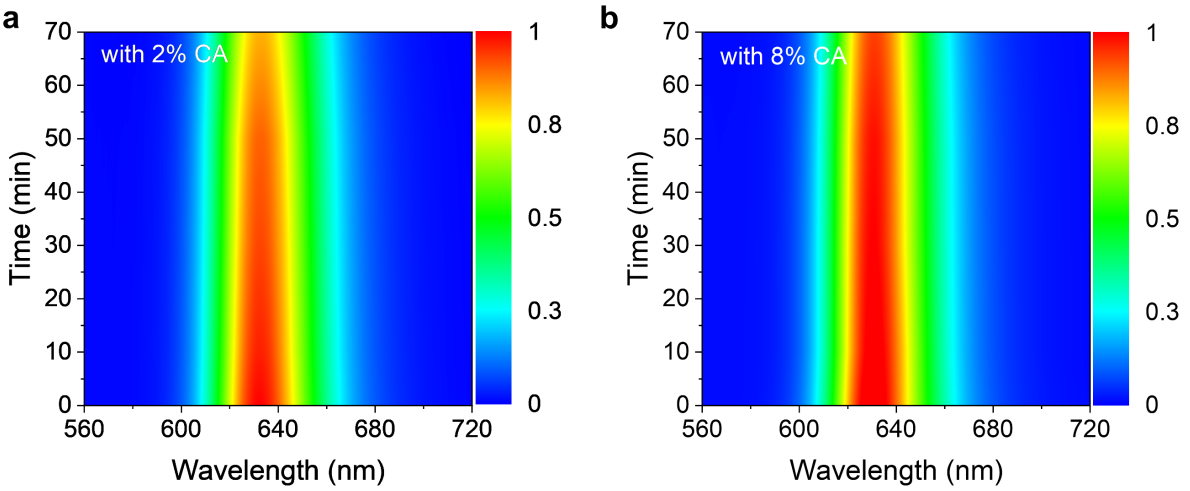

Supplementary Fig. 8 | Pseudo-color maps of time-dependent PL spectra for perovskite films. Pseudo-color maps of time-dependent PL spectra for the samples with 2% (**a**) and 8% CA (**b**).

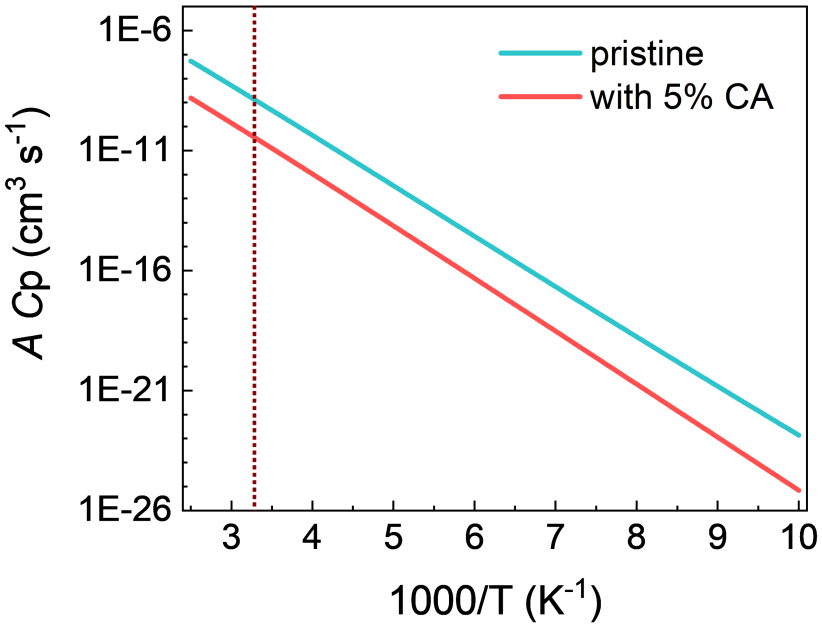

Supplementary Fig. 9 | Curves of nonradiative capture coefficients with temperature. Curves of nonradiative capture coefficients with temperature for the perovskites with and without CA. The dashed line stands for the condition under room temperature.

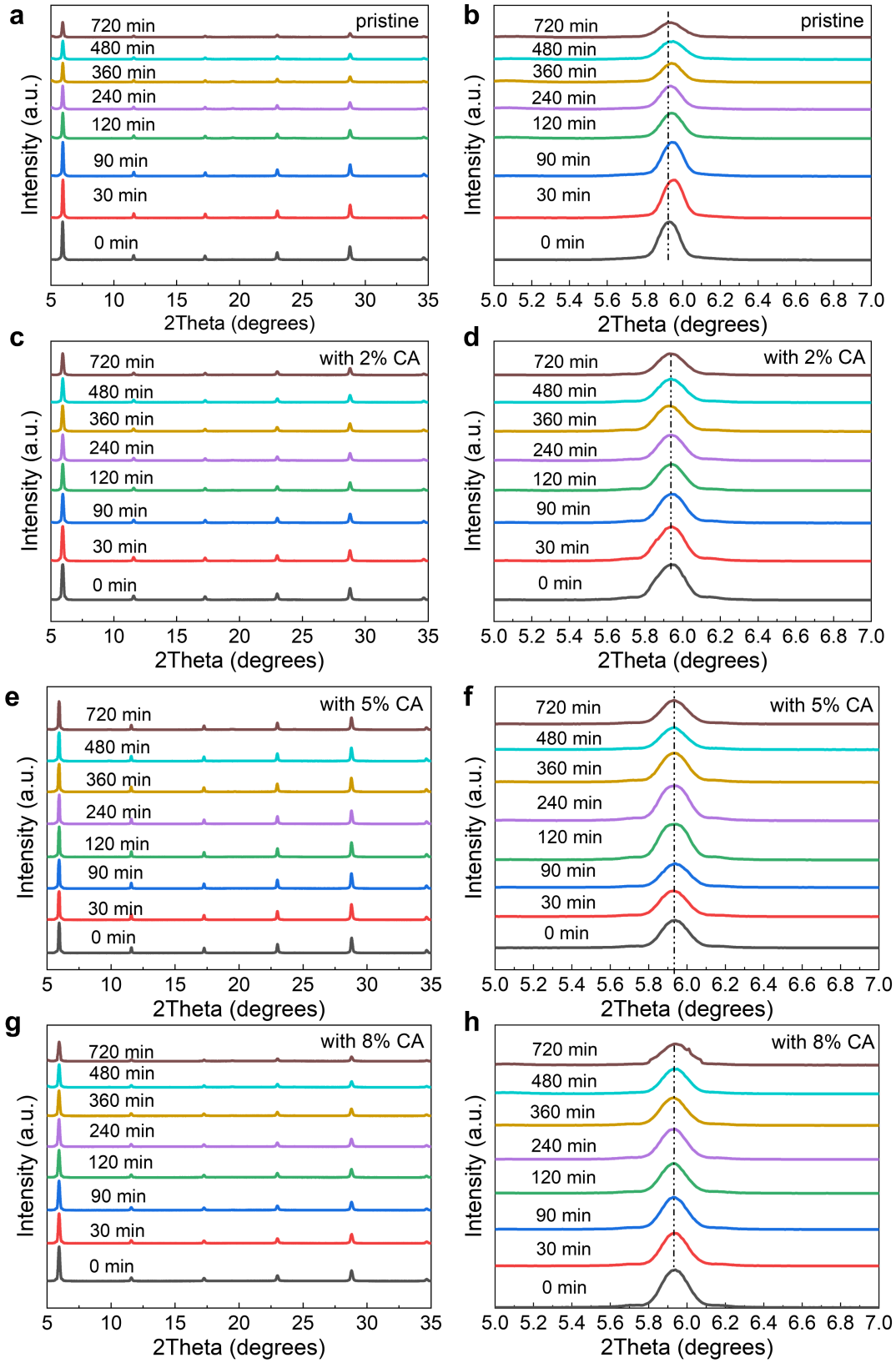

Supplementary Fig. 10 | XRD patterns of the perovskite thin films for different storage time. XRD patterns of the pristine and the films with 2%, 5% and 8% CA (**a**, **c**, **e**, **g**) for different storage time, and the corresponding curves of (002) peak (**b**, **d**, **f**, **h**).

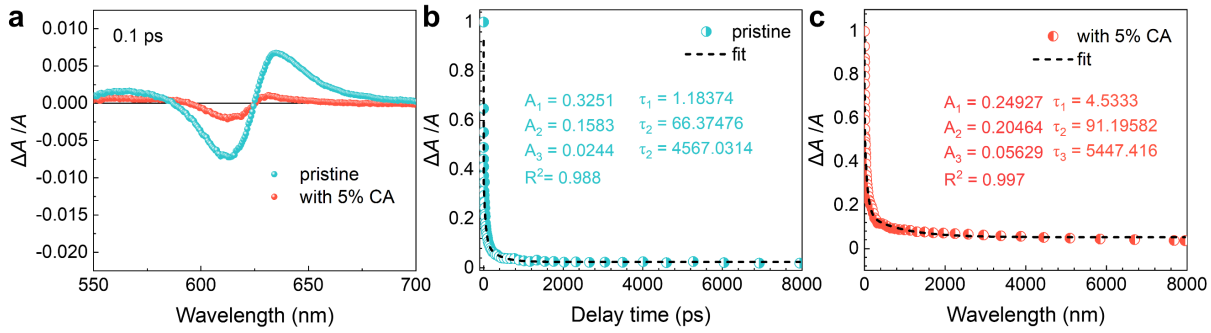

Supplementary Fig. 11 | TA signals and kinetic traces of the perovskite thin films. a, TA signals of the films with an excitation wavelength of 400 nm at a corresponding delay time of 0.1 ps. Kinetic traces at a probing wavelength of 615 nm for the films without (**b**) and with 5% CA (**c**).

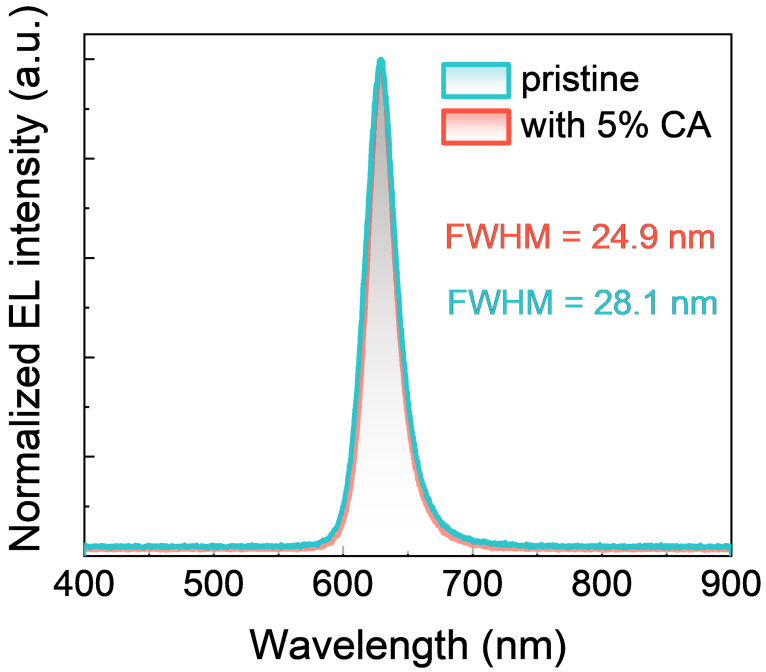

Supplementary Fig. 12 | Normalized EL spectra of the devices. Normalized EL spectra of the devices without and with 5% CA at a driving voltage of 3.5.

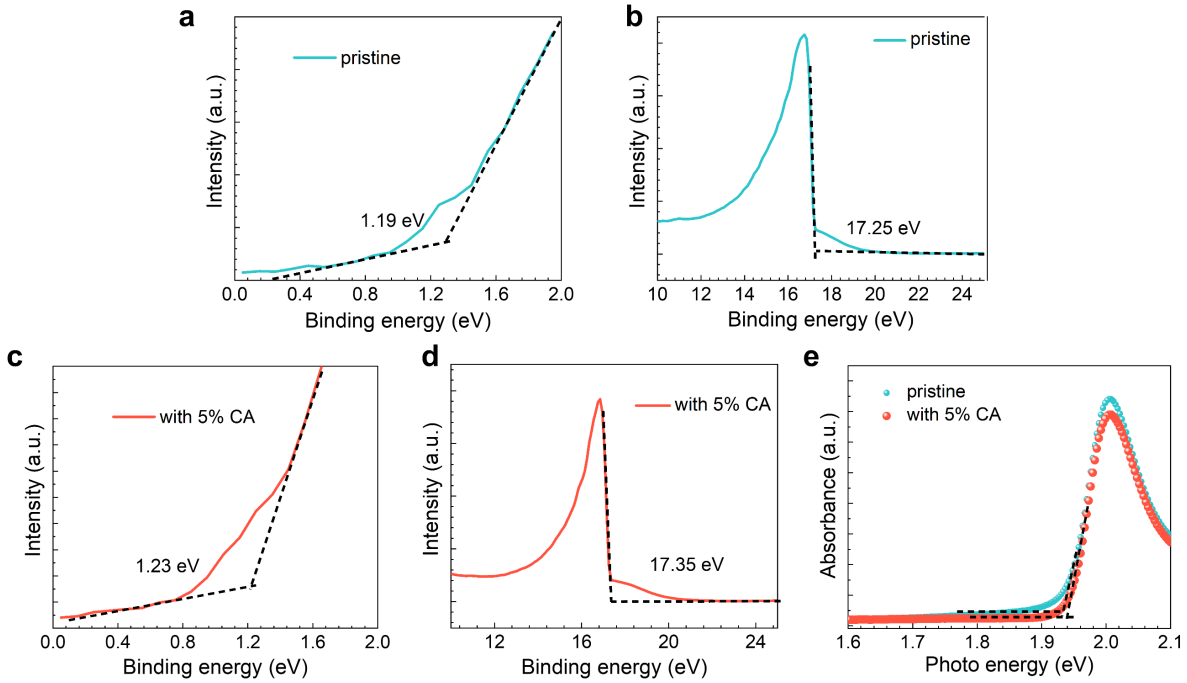

Supplementary Fig. 13 | UPS plots of the perovskite thin films. UPS results of the perovskite thin films without (**a** and **b**) and with 5% CA (**c** and **d**). **e**, On-set plots of the absorbance curves for the samples.

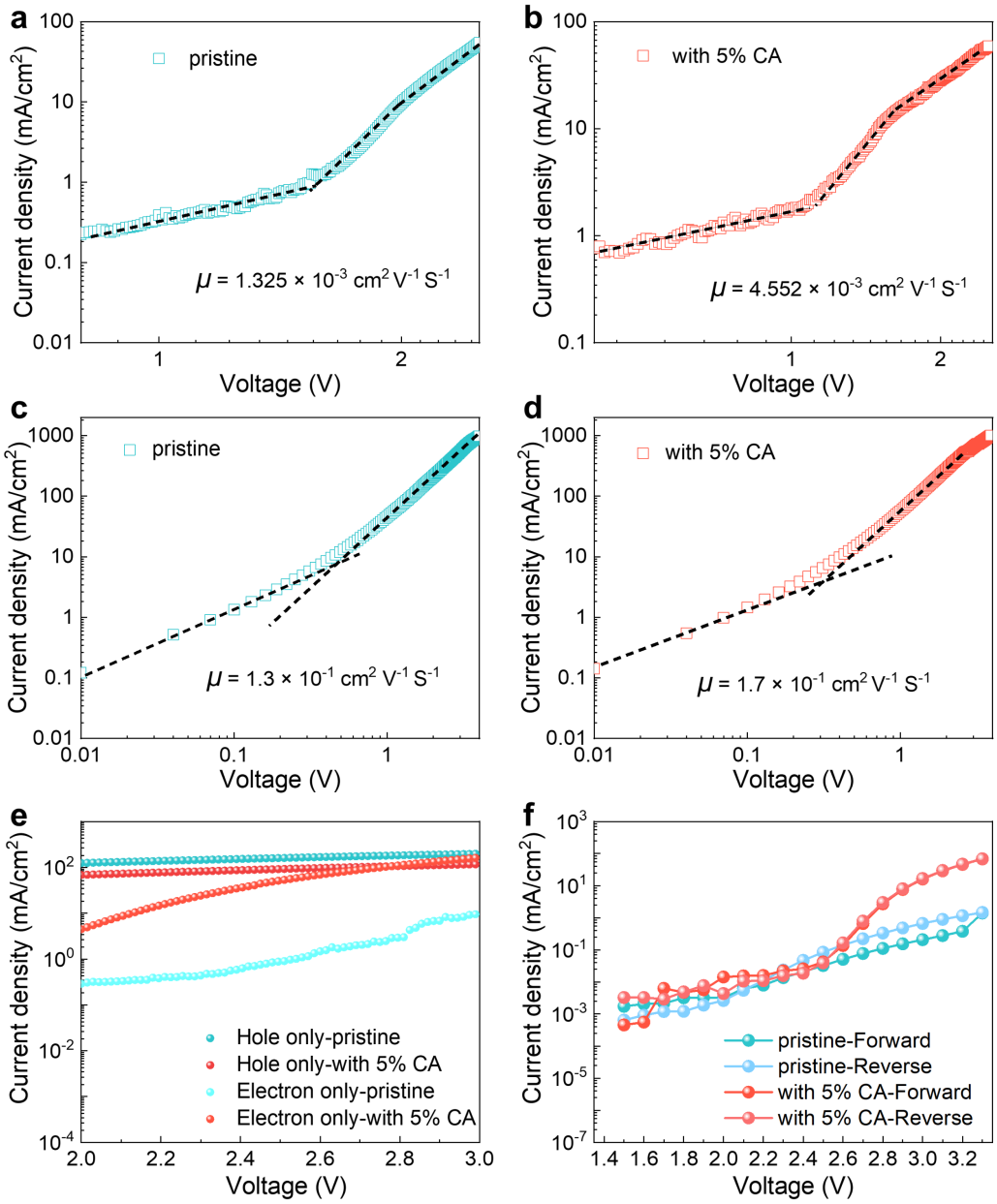

Supplementary Fig. 14 | SCLC measurements of the Sn perovskite films. The upper are the plots of the electron-only devices without (**a**) and with 5% CA (**b**), while the middle are the curves of the hole-only devices without (**c**) and with 5% CA (**d**). **e**, *J*-*V* curves of the hole-only and electron-only devices with and without CA. **f**, Plots of current density versus voltage for the devices with different scanning directions.

Supplementary Table 1 | Interaction energy of dimers and trimers normalized on the number of CA molecules. The trimer with 2 enols facing the surface and 7 ketos results as the most stable among all the possible dimers and trimers.

Dimers	4 enol – 2 keto	-0.40 eV
	2 enol – 4 keto #1	-0.75 eV
	2 enol – 4 keto #2	-0.15 eV
Trimers	5 enol – 4 keto	-0.33 eV
	4 enol – 5 keto	-0.52 eV
	2 enol – 7 keto #1	-0.91 eV
	2 enol – 7 keto #2	-0.12 eV

Supplementary Table 2 | Comparison of Bader charge transfer for the Sn perovskite films.

Atom	pristine	with 5% CA
Sn 3	0.7281	0.9629
Sn 92	0.7747	0.6436

Supplementary Table 3 | Summarized parameters from the XPS results for the Sn perovskite films.

Sample	Sn^{2+} area %	Sn^{4+} area %	I^- area %	I_2 area %	Sn/I
pristine	140920.5	36785.05	580518.5	123329.7	0.25
with 5% CA	166281.49	17658.19	788382.3	23327.3	0.23